

# Asymmetric ring-opening of epoxides on chiral Co(Salen) catalyst synthesized in SBA-16 through the “ship in a bottle” strategy

Hengquan Yang, Lei Zhang, Weiguang Su, Qihua Yang\*, Can Li\*

State Key Laboratory of Catalysis, Dalian Institute of Chemical Physics, Chinese Academy of Sciences, 457 Zhongshan Road, Dalian 116023, China

Received 4 January 2007; revised 7 March 2007; accepted 7 March 2007

Available online 24 April 2007

## Abstract

Chiral Co(Salen) complex was synthesized in the mesoporous cage of SBA-16 through the “ship in a bottle” method. The pore entrance size of SBA-16 was precisely tailored by varying the autoclaving time and silylation with phenyltrimethoxysilane to trap Co(Salen) complex in the cage of SBA-16. Chiral Co(Salen) trapped in SBA-16 shows enantioselectivity (up to 87–96% ee) as high as that of the homogeneous catalyst for the asymmetric ring opening of terminal epoxides and can be recycled at least 10 times with no apparent loss of activity. The activity for the catalyst trapped inside SBA-16 can be significantly increased when the surface is modified with organic groups. This work extends the “ship in a bottle” synthesis from microporous materials to mesoporous cage-like materials and develops an effective strategy to trap metal complex catalyst with large molecular size into the nanopores or cavities of mesoporous materials.

© 2007 Elsevier Inc. All rights reserved.

**Keywords:** Ship in a bottle; Mesoporous cage-like material; Salen catalyst; Asymmetric ring-opening

## 1. Introduction

The “ship in a bottle” synthesis has become an efficient method for immobilizing homogeneous catalysts within the solid matrix, particularly in microporous materials like zeolites [1,2]. Over the last two decades, metal complexes with ligands like Salen, porphyrin, phthalocyanine, bipyridine, triaza-cyclononane, and CO have been successfully synthesized inside the supercages of X, Y, EMT, MCM-22 zeolites, and montmorillonite for various catalytic reactions [3–19]. The pore entrance size and cage dimension of the microporous zeolites are strictly limited by their crystalline topology (usually <1.5 nm). It is difficult to synthesize the metal complex with relatively larger molecular size (like Jacobsen’s catalyst with the ligand 3,5,3’,5’-tetra-*tert*-butyl-substituted SalenH<sub>2</sub>) [6,7,20] by the “ship in a bottle” method in the cage of a zeolite, except for the cage-enlarged faujasites [20], EMT [19] and MCM-22 ze-

olite [8]. Compared with microporous zeolites, ordered mesoporous silicas have larger pore size and pore volume, which provides possibilities for trapping larger molecules and more “comfortable” microenvironment for guest molecules. Previously, Algarra and Tanamura [21,22] tried to synthesize copper phthalocyanine and porphyrin in MCM-41 through the “ship in a bottle” method, but reported no catalytic properties of the prepared catalysts. So far, the leaching of metal complexes remains a problem when metal complexes are accommodated in the mesoporous materials without modifying the pore structure.

Ordered mesoporous silicas with cage-like structures, such as SBA-1 (cubic, *Pm3n*) [23,24], SBA-16 (cubic, *Im3m*) [25,26], FDU-12 (cubic, *Fm3m*) [27], and FDU-1 (cubic, *Fm3m*) [28], have been well synthesized. These mesoporous cage-like silicas have tunable cage sizes (4–8 nm for SBA-16; 10–22 nm for FDU-12) and their cages are interconnected three-dimensionally by tunable pore entrances. The large cages of these mesoporous materials can accommodate metal complexes of large molecular size, whereas the smaller pore entrances may prevent leaching of the metal complex confined in the mesoporous cage. In addition, the existence of plentiful hydroxyl groups in the mesoporous silicas provides the possi-

\* Corresponding authors. Fax: +86 411 84694447.

E-mail addresses: [yangqh@dicp.ac.cn](mailto:yangqh@dicp.ac.cn) (Q. Yang), [canli@dicp.ac.cn](mailto:canli@dicp.ac.cn) (C. Li).

URL: <http://www.canli.dicp.ac.cn> (C. Li).

bility of tailoring the pore entrance size by a simple silylation reaction [25]. Simultaneously, the surface properties, such as hydrophobicity and hydrophilicity, can be modified by silylation using silane precursors with different organic groups.

Although mesoporous cage-like silicas are good candidates for accommodation of the metal complexes, the synthesis of metal complexes in the mesoporous cage-like materials through the “ship in a bottle” method has been rarely reported. An underlying reason for this is the difficulty in exactly tailoring and determining the pore entrance size, which is a key factor in the successful encapsulation of a metal complex through the “ship in a bottle” strategy. Our primary results indicated that homogeneous catalysts with large molecular size can be directly encapsulated in the nanocavities of mesoporous materials [29]. Herein, we investigated the “ship in a bottle” synthesis of chiral Co(Salen) inside the mesoporous cage of SBA-16 using the molecular fragments of 3,5,3',5'-tetra-*tert*-butyl-SalenH<sub>2</sub> and Co(OAc)<sub>2</sub>. Tailoring the pore entrance size via silylation is crucial to confine the metal complex. The Co(Salen) catalyst trapped inside SBA-16 (silylated with phenyltrimethoxysilane) exhibited comparable enantioselectivity to its homogeneous counterpart in the asymmetric ring-opening of the terminal epoxides. No apparent loss of activity and enantioselectivity was observed for the heterogeneous catalyst even after 10 reaction cycles.

## 2. Experimental

### 2.1. Reagents and materials

Pluronic P123 copolymer (EO<sub>20</sub>PO<sub>70</sub>EO<sub>20</sub>), phenyltrimethoxysilane (98%), and 2,2-dimethoxypropane (>99%) were purchased from Aldrich. Pluronic F127 (EO<sub>106</sub>PO<sub>70</sub>EO<sub>106</sub>) was obtained from Sigma. Tetraethylorthosilicate (TEOS, AR), epichlorohydrin (>99%), and propylene oxide (>99%) were purchased from the Shanghai Chemical Reagent Company of the Chinese Medicine Group. (*R,R*)-*N,N'*-bis(3,5-di-*tert*-butylsalicylidene)-1,2-cyclohexanediamine (denoted SalenH<sub>2</sub>) was synthesized as described previously [30].

Mesoporous cage-like material SBA-16 was synthesized according to a modified method [25]. SBA-16(4.9), SBA-16(5.4), and SBA-16(5.9) were synthesized by autoclaving at 373 K for 5.5, 9, and 12 h, respectively, where the number in parentheses is the cage size (in nanometers) of the mesoporous material analyzed from N<sub>2</sub> adsorption branch based on the BJH method.

### 2.2. Modification of SBA-16 by silylation

1.0 mL of dry toluene was added to 1.0 g of SBA-16(*n*) (evacuated at 398 K for 6 h; *n* = 4.9, 5.4, 5.9), followed by the addition of 1.25 mL of anhydrous *n*-butylamine and 5 mmol of phenyltrimethoxysilane. After refluxing at 384 K for 24 h under Ar atmosphere, the resulting solid was isolated by rapid filtration and thoroughly washed with toluene and the mixture of CH<sub>2</sub>Cl<sub>2</sub> and diethyl ether. The resultant materials were designated SBA-16(*n*)-Ph, where *n* is the cage size of SBA-16 and Ph denotes the phenyl group.

### 2.3. Synthesis of chiral Co(Salen) in the cage of SBA-16 through the “ship in a bottle” method

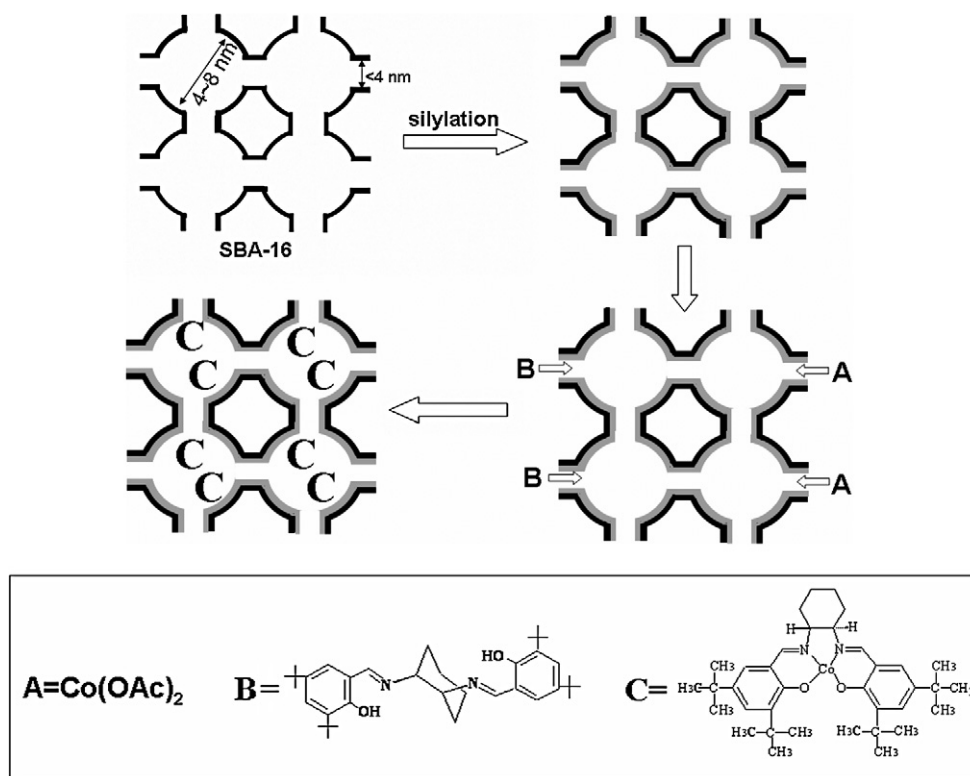
1.0 g of SBA-16(4.9) or SBA-16(*n*)-Ph (*n* = 4.9, 5.4, 5.9) and 0.15 g of SalenH<sub>2</sub> ligand were mixed together and kept at 428 K for 24 h under vacuum. After cooling to 368 K, 0.113 g of Co(OAc)<sub>2</sub>·4H<sub>2</sub>O, 15 mL of ethanol, and 7.5 mL of toluene were added. The mixture was stirred at 368 K for 24 h under Ar atmosphere. The isolated solid was thoroughly washed in a Soxhlet apparatus consecutively with CH<sub>2</sub>Cl<sub>2</sub>, THF, and ethanol. Co(Salen)/SBA-16(4.9) and Co(Salen)/SBA-16(*n*)-Ph (*n* = 4.9, 5.4, 5.9) were prepared from SBA-16(4.9) and SBA-16(*n*)-Ph (*n* = 4.9, 5.4, 5.9), respectively. The chiral Co(Salen) synthesized in SBA-16 is schematically presented in Scheme 1.

### 2.4. Catalytic reaction

The catalyst was oxidized in a mixture of toluene and acetic acid by air for 2.5 h before reaction. The solid catalyst was obtained by centrifugation and was evacuated under vacuum to remove toluene and acetic acid. For asymmetric ring-opening of epichlorohydrin, when THF was used as solvent, 2 mmol of epichlorohydrin, 0.2 g of THF, and 1.3 mol of water were mixed with the catalyst (Co content 0.02 mmol). The reaction was performed at 298 K. In the case of the reaction without solvent, the reaction was performed at 298 K with a molar ratio of epichlorohydrin:H<sub>2</sub>O:Co of 1:0.75:0.01. For asymmetric ring-opening of propylene oxide, the reaction was performed at 283 K with a molar ratio of propylene oxide:H<sub>2</sub>O:Co of 1:0.8:0.005. After reaction, 0.35 mL of THF was added to the reaction mixture, and nonane was added as an internal standard. The diol thus-obtained was derived with dimethoxypropane in the presence of *p*-toluenesulfonic acid. The derivatives were purified with short gel column and then analyzed by gas chromatography (Agilent 6890 with HP-Chiral19091G-B213 capillary column). The catalyst was isolated from the reaction mixture by centrifugation. After being washed with THF, oxidized in toluene/acetic acid by air for 2.5 h, isolated by centrifugation, and dried under vacuum, the recovered catalyst was used in the recycling experiments.

### 2.5. Characterization

Powder X-ray diffraction patterns of SBA-16 were recorded on a Rigaku D/Max3400 powder diffraction system (CuK $\alpha$ , 40 kV, 30 mA). N<sub>2</sub> physical adsorption analysis was carried out on Micromeritics ASAP 2020 volumetric adsorption analyzer. Before the adsorption measurements, the samples were outgassed at 393 K for 6 h. UV–vis spectra and diffuse-reflectance UV–vis spectra were recorded on a JASCOV-550 UV–vis spectrophotometer using dichloromethane and BaSO<sub>4</sub> as the reference, respectively. FT-IR spectra were collected on a Thermo Nicolet Nexus 470 infrared spectrometer, and Co content was analyzed on a Plasma-spec-II (Leeman). TEM micrographs were taken using a JEM-2010 transmission electron microscopy at an acceleration voltage of 120 kV.



Scheme 1. Schematic description of chiral Co(Salen) synthesized in the cages of phenyl-modified SBA-16 through the “ship in a bottle” method.

### 3. Results and discussion

#### 3.1. Tuning the pore entrance size of SBA-16

To obtain mesoporous cage-like silicas with different pore entrance sizes, SBA-16(4.9), SBA-16(5.4), and SBA-16(5.9) (with 4.9, 5.4, and 5.9 designating cage sizes (in nm) of these three materials) were synthesized as described previously [25]. Fig. 1 shows the XRD patterns of these materials. All materials exhibit two diffraction (110) and (200) peaks, characteristic of mesoporous materials with the cubic  $Im\bar{3}m$  structure. The  $2\theta$  value of the (110) diffraction peak gradually shifts to lower angle from SBA-16(4.9) to SBA-16(5.9), suggesting that the materials with larger unit cells can be obtained with longer autoclaving time.

The  $\text{N}_2$  sorption isotherms of SBA-16(4.9), SBA-16(5.4), and SBA-16(5.9) are displayed in Fig. 2. The sorption plots show a typical H2 hysteresis loop characteristic of materials with a good-quality cage-like porous structure. The cage size also increases with increasing autoclaving time (Table 1).

The pore entrance size is very important for the successful synthesis of metal complexes in the cage of SBA-16 through the “ship in a bottle” method. In principle, the pore entrance size should be larger than the molecular size of the fragments used for constructing the metal complex and smaller than the metal complex catalyst formed inside the cage. In this work, we chose chiral Co(Salen) as a model metal complex, and synthesized Co(Salen) complex in the cage of SBA-16 through the flexible ligand method [9]. The process of synthesizing Co(Salen) in the cage of SBA-16 is schematically displayed in Scheme 1.

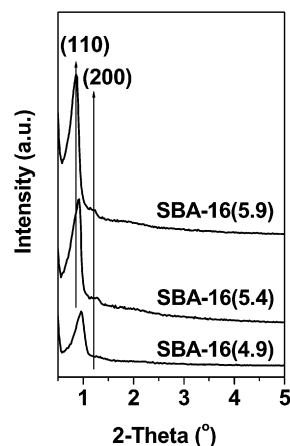


Fig. 1. XRD patterns of mesoporous SBA-16 materials available for trapping metal complex catalysts.

The chiral ligand (SalenH<sub>2</sub>) with flexible structure can easily twist its way to diffuse through the pore entrance into the cage (at 428 K). Once SalenH<sub>2</sub> in the cage coordinates with  $\text{Co}(\text{OAc})_2 \cdot 4\text{H}_2\text{O}$ , Co(II)(Salen) with a rigid structure can be formed, and thus it cannot diffuse out from the mesoporous cage if the pore entrance size is smaller than the molecular size of Co(II)(Salen).

However, it is difficult to estimate the pore entrance size (<math><4\text{ nm}</math>) only from the desorption branch of  $\text{N}_2$  sorption isotherms, due to the intrinsic  $\text{N}_2$  capillary evaporation [31]. To date, two methods for determining the pore entrance size of mesoporous cage-like materials have been reported [32,33]. One of these methods is extensive high-resolution transmis-

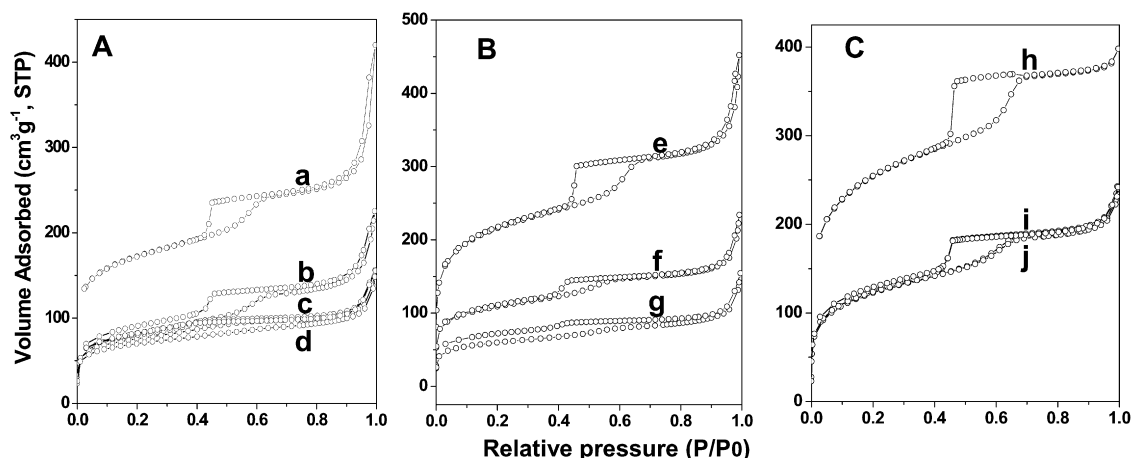


Fig. 2.  $N_2$  sorption isotherms of (a) SBA-16(4.9); (b) Co(Salen)/SBA-16(4.9); (c) SBA-16(4.9)-Ph; (d) Co(Salen)/SBA-16(4.9)-Ph; (e) SBA-16(5.4); (f) SBA-16(5.4)-Ph; (g) Co(Salen)/SBA-16(5.4)-Ph; (h) SBA-16(5.9); (i) SBA-16(5.9)-Ph; and (j) Co(Salen)/SBA-16(5.9)-Ph.

Table 1

Surface area, pore volume and cage diameter of the cage-like materials from  $N_2$  sorption analysis

Mesoporous materials	Surface area (m <sup>2</sup> /g)	Pore volume <sup>a</sup> (cm <sup>3</sup> /g)	Cage diameter <sup>b</sup> (nm)
SBA-16(4.9)	755	0.65	4.9
Co(Salen)/SBA-16(4.9)	287	0.35	4.9
SBA-16(4.9)-Ph	257	0.24	3.3
Co(Salen)/SBA-16(4.9)-Ph	238	0.24	3.4
SBA-16(5.4)	748	0.70	5.4
SBA-16(5.4)-Ph	377	0.35	4.4
Co(Salen)/SBA-16(5.4)-Ph	207	0.24	4.3
SBA-16(5.9)	892	0.61	5.9
SBA-16(5.9)-Ph	432	0.37	5.2
Co(Salen)/SBA-16(5.9)-Ph	433	0.37	5.2

<sup>a</sup> Single point pore volume calculated at relative pressure  $P/P_0$  of 0.99.

<sup>b</sup> BJH method from adsorption branch.

sion electron microscopy imaging from different directions. However, this method is currently applicable only for three-dimensional ordered materials with sufficiently large ordered domains. The other method is an indirect method based on monitoring pore accessibility after modification of the pore surface with different-sized molecules. This method can give a range of pore entrance sizes rather than an exact value.

Herein we propose an easy method for estimating the pore entrance size whether it is larger or smaller than a probe molecule, based on an absorption method using Co(II)(Salen) as a probe molecule. When Co(II)(Salen) in  $CH_2Cl_2$  solution is absorbed into the cage of SBA-16 material, the concentration of Co(II)(Salen) in the filtrate should be decreased, and the concentration change can be monitored by UV–vis spectroscopy. UV–vis spectra of the filtrates after absorption with SBA-16(4.9), SBA-16(5.4), and SBA-16(5.9) are shown in Fig. 3. The UV–vis spectrum of the Co(II)(Salen) in  $CH_2Cl_2$  exhibits bands at 360 and 420 nm. After absorption with SBA-16(5.4) and SBA-16(5.9), the intensities of the bands are dramatically decreased, indicating that the pore entrance size of SBA-16(5.4) and SBA-16(5.9) is larger than the molecular size of Co(II)(Salen). After absorption with SBA-16(4.9), the intensities of the characteristic bands of Co(II)(Salen) de-

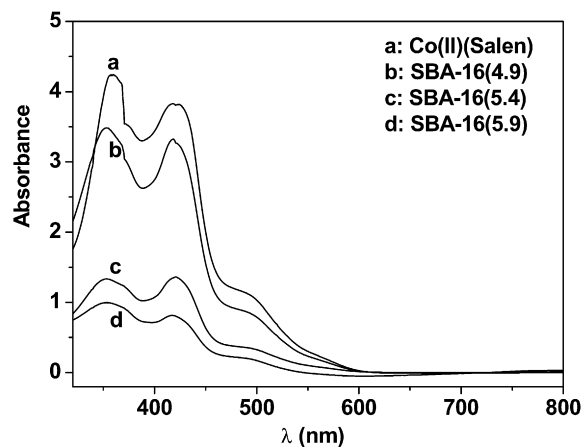


Fig. 3. UV–vis spectra of Co(II)(Salen) solution in dichloromethane absorbed with cage-like materials. Absorption experiment protocol is as followed: 0.08 g of SBA-16 materials were dispersed in 3.8 mL of  $CH_2Cl_2$  containing  $3.3 \times 10^{-6}$  mol of (*R,R*)-Co(Salen)(II). The mixture was stirred in a sealed tube for 5 h. After centrifugation, the solution was measured with UV–vis spectroscopy.

creased only slightly. This result shows that the dominating entrance size of SBA-16(4.9) is smaller than the molecular size of Co(II)(Salen). This is in good agreement with the conclusion of Jaroniec et al. [25] that the pore entrance size increases with autoclaving time. The results of the UV–vis experiments show that only the pore entrance size of SBA-16(4.9) is suitable for encapsulation of Co(II)(Salen) within the mesoporous cage. Therefore, the pore entrance sizes of SBA-16(5.4) and SBA-16(5.9) were further tuned by silylation with phenyltrimethoxysilane.

The  $N_2$  sorption isotherms of SBA-16(5.4)-Ph and SBA-16(5.9)-Ph (silylated with phenyltrimethoxysilane) exhibit type IV isotherm patterns with H2 hysteresis loops, confirming that the cage-like structure of SBA-16(5.4) and SBA-16(5.9) was maintained after the silylation (also shown in Figs. 2B and 2C, respectively). For comparison, SBA-16(4.9) was also silylated with phenyltrimethoxysilane. The  $N_2$  sorption isotherm of SBA-16(4.9)-Ph is of type I (Fig. 2A). After silylation, the surface area, pore volume, and pore size of SBA-16(*n*) appar-

ently decreased (Table 1). This confirms that the phenyl group was grafted on the surface of SBA-16. FT-IR spectra of SBA-16(5.4) and SBA-16(5.4)-Ph are presented in Fig. 4. Compared with SBA-16(5.4), SBA-16(5.4)-Ph exhibits additional peaks at 3078, 3058, and 1434  $\text{cm}^{-1}$ . The peaks at 3078 and 3058  $\text{cm}^{-1}$  are attributed to the C–H stretching vibrations of phenyl group. The peak at 1434  $\text{cm}^{-1}$  can be assigned to C=C stretching vibration of phenyl group. The IR results further confirm successful grafting of a phenyl group in SBA-16 by silylation.

UV–vis spectra of the filtrate after absorbing Co(II)(Salen) with SBA-16(4.9)-Ph, SBA-16(5.4)-Ph, SBA-16(5.9)-Ph are shown in Fig. 5. After absorption with SBA-16(4.9)-Ph and SBA-16(5.4)-Ph, the intensities of the bands at 360 and 420 nm remain almost the same as that of the initial solution of Co(II)(Salen) in  $\text{CH}_2\text{Cl}_2$ . This indicates that the pore entrance size of these materials is small enough to prevent diffusion of the probe molecule through the pore entrance. These results show that silylation is an efficient method of reducing the pore entrance size of SBA-16. When SBA-16(5.9)-Ph is used as the absorbent, the intensity is dramatically reduced. This suggests that the pore entrance size of SBA-16(5.9)-Ph is still larger than the molecular size of Co(II)(Salen). Thus, a silane precursor

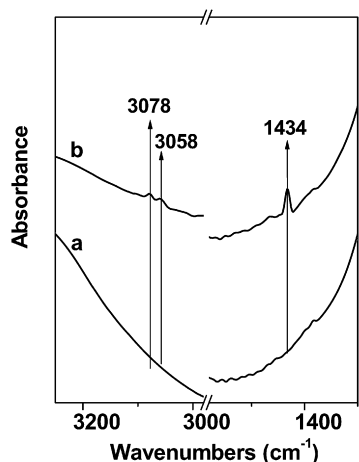


Fig. 4. FT-IR spectra of (a) SBA-16(5.4) and (b) SBA-16(5.4)-Ph (modified with phenyl group).

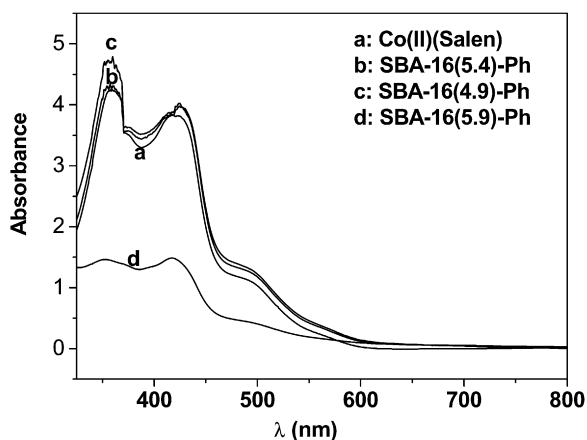


Fig. 5. UV–vis spectra of Co(II)(Salen) in dichloromethane solution absorbed with cage-like materials. Absorption experiment is the same as that in Fig. 3.

with a bulkier group is needed to reduce the pore entrance size of SBA-16(5.9) to less than the molecular size of Co(Salen). The foregoing results indicate that SBA-16(4.9), SBA-16(4.9)-Ph, and SBA-16(5.4)-Ph may be suitable host materials for trapping Co(Salen) in the mesoporous cage.

### 3.2. Synthesis of Co(Salen) in the cage of SBA-16 through the “ship in a bottle” method

Co(Salen) was synthesized in the mesoporous cage of SBA-16 using SalenH<sub>2</sub> and Co(OAc)<sub>2</sub>·4H<sub>2</sub>O through the “ship in a bottle” method, as illustrated in Scheme 1. The formation of Co(Salen) in SBA-16 was verified using FT-IR and UV–vis spectroscopy. The FT-IR spectra of SalenH<sub>2</sub>, Co(II)(Salen), Co(Salen)/SBA-16(4.9), and Co(Salen)/SBA-16(5.4)-Ph are shown in Fig. 6. The FT-IR spectrum of Co(II)(Salen) shows the C–H stretching vibrations at 2956 and 2866  $\text{cm}^{-1}$  and C–H bending vibrations at 1384 and 1360  $\text{cm}^{-1}$ . The characteristic vibration of Co(II)(Salen) was found at 1530  $\text{cm}^{-1}$ . SalenH<sub>2</sub> gives the C–H stretching vibrations only at 3000–2800  $\text{cm}^{-1}$  and bending vibrations at 1400–1300  $\text{cm}^{-1}$ . In the FT-IR spectra of Co(Salen)/SBA-16(4.9) and Co(Salen)/SBA-16(5.4)-Ph, the stretching vibrations of C–H at 2956 and 2866  $\text{cm}^{-1}$  and the characteristic C=N vibration at 1530  $\text{cm}^{-1}$  are clearly observed, similar to Co(II)(Salen). The bending vibrations of C–H were also found at 1400–1300  $\text{cm}^{-1}$  with a slight blue shift. The FT-IR results demonstrate the formation of Co(II)(Salen) inside SBA-16(4.9) and SBA-16(5.4)-Ph through the “ship in a bottle” method. The FT-IR spectrum of Co(Salen)/SBA-16(5.4)-Ph clearly shows the C–H vibration of Ph group at 3078 and 3058  $\text{cm}^{-1}$ , further confirming the existence of phenyl group on SBA-16 after the “ship in a bottle” synthesis. No characteristic vibration of Co(Salen) was found in the FT-IR spectra of Co(Salen)/SBA-16(4.9)-Ph and Co(Salen)/SBA-16(5.9)-Ph (data not shown); this indicates that almost no Co(II)(Salen) exists in SBA-16(4.9)-Ph and SBA-16(5.9)-Ph.

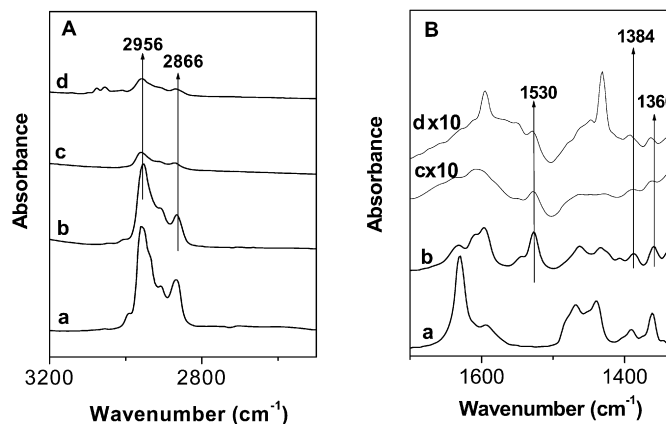


Fig. 6. FT-IR spectra of (a) SalenH<sub>2</sub>; (b) Co(II)(Salen); (c) Co(Salen)/SBA-16(4.9); and (d) Co(Salen)/SBA-16(5.4)-Ph. (The spectra were recorded after heating the samples at 523 K for 3 h under vacuum.) (A) The spectra between 2500 and 3200  $\text{cm}^{-1}$ ; (B) the magnified spectra between 1350 and 1700  $\text{cm}^{-1}$ .

Co(Salen)/SBA-16(4.9) and Co(Salen)/SBA-16(5.4)-Ph were further characterized by UV–vis spectroscopy (Fig. 7). The UV–vis spectrum of Co(II)(Salen) in CH<sub>2</sub>Cl<sub>2</sub> shows three bands at 360 (the  $\pi$ – $\pi^*$  transition of C=N), 420, and 495 nm ( $d$ – $\pi^*$  transition) (Fig. 7). Similar to Co(II)(Salen), three bands at 345, 420, and 495 nm were also found in the UV–vis spectra of Co(Salen)/SBA-16(5.4)-Ph. (SBA-16(5.4)-Ph shows only one band at 262 due to the phenyl group; b of Fig. 7). This further confirms that Co(II)(Salen) was formed inside the cage of SBA-16(5.4)-Ph. For Co(Salen)/SBA-16(4.9), only a broad band at around 380 nm was observed instead of the three well-defined bands, similar to the Co(Salen) loaded on MCM-41 by the adsorption method [34]. This may be due to the strong interaction between Co(Salen) and the surface hydroxyl group of unmodified SBA-16(4.9) [35]. Compared with the free Co(II)(Salen) in solution, only a slight blue shift of the band due to the  $\pi$ – $\pi^*$  transition of C=N (from 360 to 345 nm) was observed for Co(Salen)/SBA-16(5.4)-Ph. The foregoing results probably indicate that surface modification by a Ph group can greatly reduce the strong interaction of Co(Salen) with the hydrophilic microenvironment of SBA-16. Compared with

SBA-16(4.9), SBA-16(5.4)-Ph can provide a microenvironment for Co(Salen) more akin to that in solution.

The mesostructure of Co(Salen)/SBA-16(5.4)-Ph was characterized by XRD and TEM. The small angle X-ray diffraction pattern of Co(Salen)/SBA-16(5.4)-Ph still exhibits (110) and (200) diffractions of a cubic  $Im\bar{3}m$  structure (Fig. 8A). TEM image of Co(Salen)/SBA-16(5.4)-Ph is shown in Fig. 8B. The (110) projection corresponding to cubic  $Im\bar{3}m$  structure indicates that the mesoporous structure of SBA-16(5.4) was maintained after the “ship in a bottle” synthesis.

The pore volume and surface area of Co(Salen)/SBA-16(4.9) and Co(Salen)/SBA-16(5.4)-Ph are sharply decreased (Table 1) compared with the parent materials SBA-16(4.9) and SBA-16(5.4)-Ph. This could be attributed to the decreased cage space due to the existence of Co(Salen) in the mesoporous cage. The N<sub>2</sub> sorption isotherms of Co(Salen)/SBA-16(4.9)-Ph and Co(Salen)/SBA-16(5.9)-Ph are almost overlapped with their parent materials SBA-16(4.9)-Ph and SBA-16(5.9)-Ph (Figs. 2A and 2C). In addition, the surface area and pore volume of SBA-16(4.9)-Ph and SBA-16(5.9)-Ph remain almost the same before and after the “ship in a bottle” synthesis (Table 1), indicating that few Co(Salen) molecules exist inside the cages, consistent with the results of FT-IR and UV–vis characterization. Moreover, the adsorption and desorption branches of N<sub>2</sub> sorption isotherm of Co(Salen)/SBA-16(5.4)-Ph do not close at low relative pressure ( $P/P_0 < 0.4$ ). That is a common phenomenon often observed in the case of mesoporous silicas containing large amounts of organic species [25].

The results of FT-IR, UV–vis, and N<sub>2</sub> sorption analysis show that the chiral Co(Salen) exists in the mesoporous cages of SBA-16(4.9) and SBA-16(5.4)-Ph. The pore entrance size of SBA-16(4.9)-Ph is smaller than the molecular size of Co(Salen). Therefore, the fact that no Co(Salen) was formed in the cage of SBA-16(4.9)-Ph probably indicates that the pore entrance size of SBA-16(4.9)-Ph is also smaller than the molecular size of SalenH<sub>2</sub>. For SBA-16(5.9)-Ph, the metal complex formed in the cage of SBA-16(5.9)-Ph is almost washed off during the synthesis process, because the pore entrance size of SBA-16(5.9)-Ph is too large to confine Co(Salen) within the mesoporous cage, as evidenced by the absorption results.

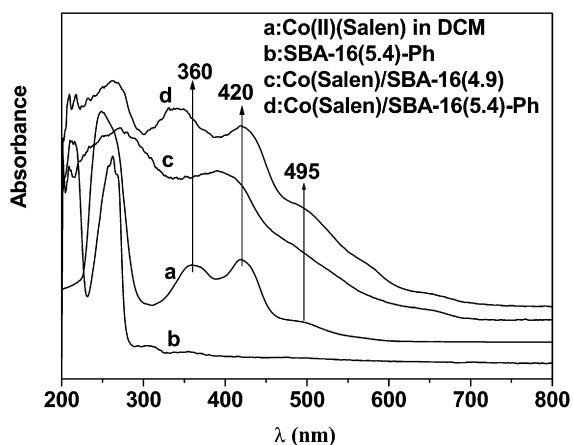


Fig. 7. UV–vis spectra of Co(II)(Salen) in CH<sub>2</sub>Cl<sub>2</sub> (DCM), Co(Salen)/SBA-16(4.9), SBA-16(5.4)-Ph (diffusion reflection), and Co(Salen)/SBA-16(5.4) (diffusion reflection).

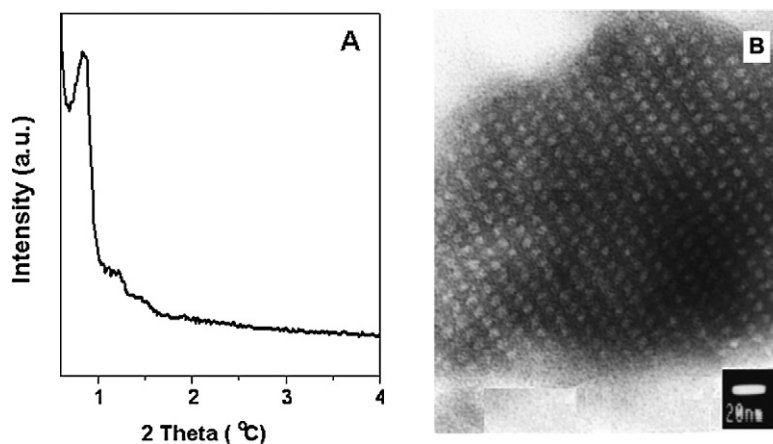


Fig. 8. XRD pattern and TEM image of SBA-16 after synthesis of Co(Salen) in SBA-16. (A) XRD pattern of Co(Salen)/SBA-16(5.4)-Ph; (B) TEM image of Co(Salen)/SBA-16(5.4)-Ph.

The pore entrance size of mesoporous cage-like material determines the synthesis of metal complex in the mesoporous cage successfully or not through the “ship in a bottle” method. The pore entrance size should be varied depending on the molecular size of the metal complex and the fragment for constructing the metal complex.

### 3.3. Asymmetric ring-opening of epoxides catalyzed by Co(Salen)/SBA-16 synthesized through the “ship in a bottle” method

The performances of catalysts prepared through the “ship in a bottle” strategy were tested in the asymmetric ring-opening of epoxides [36,37]. Before the reaction, the Co(II)(Salen) accommodated in SBA-16 was oxidized to Co(III)(Salen)(OAc) in the presence of acetic acid under air (as described in Section 2). The activities and enantioselectivities were summarized in Table 2.

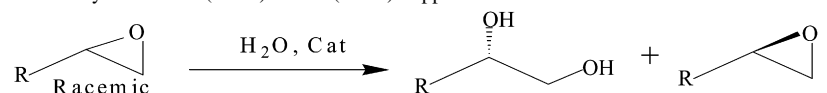
The asymmetric ring-opening of propylene oxide was carried out under solvent-free conditions. For Co(Salen)/SBA-16(4.9), only 3% diol yield with 86% ee was obtained. The activity and enantioselectivity are lower than that of the homogeneous Co(Salen) (Jacobsen catalyst) (Table 2, entry 1). However, for Co(Salen)/SBA-16(5.4)-Ph, 50% diol yield with 96% ee is obtained under identical reaction conditions. The isolated yield can reach 45% (Table 2, entry 4). Although the activity of Co(Salen)/SBA-16(5.4)-Ph is slightly lower than that of its homogeneous counterpart, the enantioselectivities of the two catalysts are similar. Very low activity is observed on Co(Salen)/SBA-16(4.9)-Ph, while Co(Salen)/SBA-16(5.9)-Ph shows a diol yield of 10% with 96% ee due to the Co(Salen) residue remaining in SBA-16(5.9)-Ph. These catalytic results are consistent with the foregoing characterization results, in-

dicating that nearly no metal complex was trapped in SBA-16(4.9)-Ph and SBA-16(5.9)-Ph.

The activity and enantioselectivity of Co(Salen)/SBA-16(4.9) are much lower than those of Co(Salen)/SBA-16(5.4)-Ph. During the catalytic reaction, the Co(Salen)/SBA-16(4.9) catalyst aggregated together and could not be well dispersed in the reaction system even under vigorous stirring. In contrast, Co(Salen)/SBA-16(5.4)-Ph can be well dispersed in the reaction system under the reaction conditions. This difference probably results from the different surface properties of Co(Salen)/SBA-16(4.9) and Co(Salen)/SBA-16(5.4)-Ph. The surface of Co(Salen)/SBA-16(4.9) without organic modification is relatively hydrophilic, hindering its dispersion in lipophilic propylene oxide. In contrast, the surface hydrophobicity of Co(Salen)/SBA-16(5.4)-Ph is greatly increased after modification with phenyl group, which makes them “dissolve” into propylene oxide. The enhanced hydrophobicity may account in part for the significantly improved catalytic activity of Co(Salen)/SBA-16(5.4)-Ph. Therefore, we can see that the catalytic performance of Co(Salen) trapped in the mesoporous cage through the “ship in a bottle” method is greatly dependent on the surface properties of the host materials. Of course, the different host–guest interaction imposed by SBA-16 and modified SBA-16 also may affect the reactivity.

The catalytic properties of the catalysts also were examined in the asymmetric ring-opening of epichlorohydrin. In solvent-free conditions, Co(Salen)/SBA-16(4.9) gave higher activity (28% diol yield with 88% ee) in the ring-opening of epichlorohydrin. Co(Salen)/SBA-16(4.9) could be well dispersed in epichlorohydrin. This differs from the case of propylene oxide, because epichlorohydrin is relatively hydrophilic in comparison with propylene oxide. As expected, Co(Salen)/SBA-16(5.4)-

Table 2  
Asymmetric ring-opening of epoxides catalyzed with Co(Salen) and Co(Salen) trapped in SBA-16



Entry	R	Catalysts	Solvent	Time (h)	Diol <sup>a</sup> (yield%)	Diol <sup>b</sup> (% ee)
1	CH <sub>3</sub>	Co(Salen) (Jacobsen catalyst) <sup>c</sup>	–	12–14	45	99
2		Co(Salen)/SBA-16(4.9)	–	20	3	86
3		Co(Salen)/SBA-16(4.9)-Ph <sup>d</sup>	–	20	Trace	
4		Co(Salen)/SBA-16(5.4)-Ph	–	20	50 (45 <sup>e</sup> )	96
5		Co(Salen)/SBA-16(5.9)-Ph <sup>d</sup>	–	20	10	96
6	CH <sub>2</sub> Cl	Co(Salen)/SBA-16(4.9)	–	20	28	88
7		Co(Salen)/SBA-16(5.4)-Ph	–	15	45	87
8		Co(Salen) (Jacobsen catalyst) <sup>f</sup>	THF	12–14	40	95
9		Co(Salen)/SBA-16(4.9)	THF	20	23	89
10		Co(Salen)/SBA-16(4.9)-Ph <sup>d</sup>	THF	20	Trace	
11		Co(Salen)/SBA-16(5.4)-Ph	THF	20	46	87
12		Co(Salen)/SBA-16(5.9)-Ph <sup>d</sup>	THF	20	7	87
13		Co(Salen)/SBA-16(5.4)-Ph (5th) <sup>g</sup>	THF	23	40	92

<sup>a</sup> Diol yield, GC analysis.

<sup>b</sup> From GC analysis, derived with dimethoxypropane in the presence of *p*-toluenesulfonic acid.

<sup>c</sup> Data obtained from Ref. [37], 0.2 mol% equiv of catalyst, 0.45 mol equiv of H<sub>2</sub>O, room temperature.

<sup>d</sup> The weight of solid catalyst is the same to Co(Salen)/SBA-16(5.4)-Ph.

<sup>e</sup> The isolated yield.

<sup>f</sup> Data obtained from Ref. [37], 0.5 mol% cat, 0.45 mol equiv of H<sub>2</sub>O, THF as a solvent.

<sup>g</sup> The fifth run of Co(Salen)/SBA-16(5.4)-Ph.

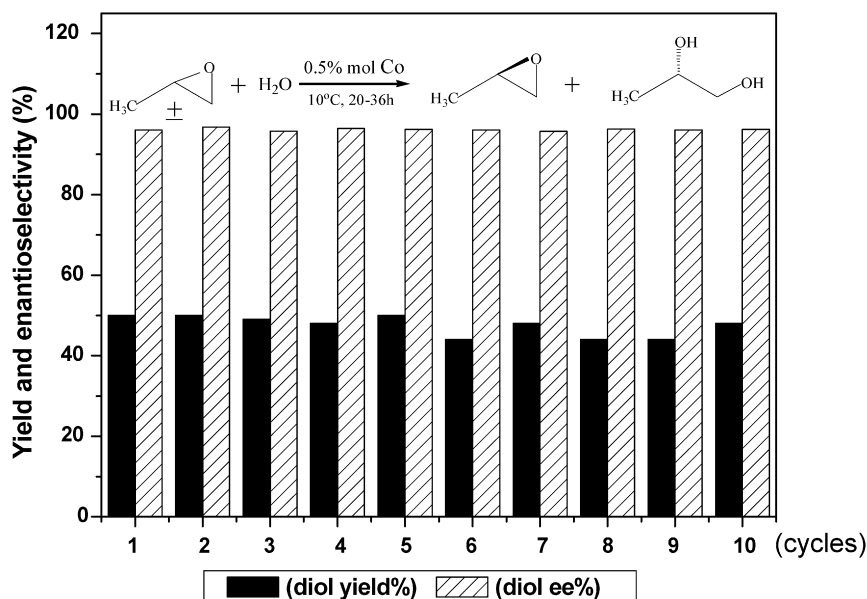


Fig. 9. Recycle test of Co(Salen)/SBA-16(5.4)-Ph in asymmetric ring-opening of propylene oxide.

Ph could also “dissolve” in solvent-free conditions and gave a 45% diol yield with 87% ee after 15 h in the asymmetric ring-opening of epichlorohydrin. The catalytic results indicate that the degree of dispersion of the solid catalyst in the reaction mixture has a direct effect on catalytic activity.

THF is usually a good solvent for the homogeneous asymmetric ring-opening of epichlorohydrin [37]. With THF as the solvent, the asymmetric ring-opening of epichlorohydrin with Co(Salen)/SBA-16(4.9) gives a 23% diol yield with 89% ee after 20 h. Co(Salen)/SBA-16(5.4)-Ph shows a 46% diol yield with 87% ee under similar conditions. The activity of Co(Salen)/SBA-16(5.4)-Ph is higher than that of Co(Salen)/SBA-16(4.9). The increased activity may be attributed to the improved surface hydrophobicity of Co(Salen)/SBA-16(5.4)-Ph and the reduced interaction of Co(Salen) with host materials, SBA-16(5.4)-Ph. Co(Salen)/SBA-16(4.9)-Ph and Co(Salen)/SBA-16(5.9)-Ph still exhibits low activity, as in the case of propylene oxide. The catalytic activity of the solid catalysts is lower with THF as solvent than without THF. This may be explained by the diffusion competition of the solvent and the substrate.

The stability of Co(Salen)/SBA-16(5.4)-Ph was investigated in the asymmetric ring-opening of propylene oxide (Fig. 9). The enantioselectivity of the recovered Co(Salen)/SBA-16(5.4)-Ph remains almost constant (96% ee) even after the ninth recycling. The activity of the recovered Co(Salen)/SBA-16(5.4)-Ph is slightly decreased compared with that of the fresh one. The decreased activity is due in part to the loss of solid catalysts during the recycling process.

Co(Salen)/SBA-16(5.4)-Ph also can be recovered efficiently for the ring-opening of epichlorohydrin in THF (Table 2). For the fifth run of the catalyst, a 40% diol yield with 92% ee still can be obtained. No apparent loss of activity and enantioselectivity was observed, confirming that Co(Salen)/SBA-16(5.4)-Ph has high stability during the catalytic process. To further confirm that the reaction was catalyzed by the heterogeneous cat-

alyst, we added extra epichlorohydrin to the filtrate after the removal of Co(Salen)/SBA-16(5.4)-Ph and found that no more diol is produced under identical conditions.

#### 4. Conclusion

The chiral metal complex Co(Salen) was accommodated in the cage-like mesoporous material SBA-16, using the “ship in a bottle” strategy. Fine-tuning of the pore entrance size of the mesoporous cage-like silica was found to be the key factor for successful trapping of Co(Salen) in the cage of the mesoporous materials. The pore entrance size of SBA-16 can be modified by a silylation reaction according to the molecular sizes of Co(Salen) catalyst, reactants, and products. Chiral Co(Salen) trapped in SBA-16 exhibits a 50% diol yield with 96% ee and a 46% diol yield with 87% ee for the asymmetric ring-opening of propylene oxide and epichlorohydrin, respectively. The enantioselectivity for the solid catalyst is comparable to that for the homogeneous counterpart. Meanwhile, the silylation reaction also can modify the inner surface properties of SBA-16. The activity for the catalyst trapped inside SBA-16 can be increased significantly when the surface of SBA-16 is modified with organic groups. No significant decrease in activity or enantioselectivity was observed even after ten cycles of the solid catalyst in the asymmetric ring-opening of propylene oxide. The “ship in a bottle” strategy, combined with tailoring the pore entrance size and modifying the surface properties of mesoporous cage-like material, is a promising method for preparing efficient and stable heterogeneous catalysts.

#### Acknowledgments

This work was supported by the National Natural Science Foundation of China (grants 20321303 and 20673113), the National Basic Research Program of China (grant 2003CB615803), Programme for Strategic Scientific Alliances between the China



and the Netherlands (2004CB720607) and the Knowledge Innovation Program of the Chinese Academy of Science (grant DICP K2006B2).

## References

- [1] N. Herron, *Inorg. Chem.* 25 (1986) 4714.
- [2] A. Corma, H. García, *Eur. J. Inorg. Chem.* 6 (2004) 1143.
- [3] P.P. Knops-Gerrits, D.D. Vos, F.T. Thibault-Starzyk, P.A. Jacobs, *Nature* 369 (1994) 543.
- [4] D.E. Devos, J.L. Meinershagen, T. Bein, *Angew. Chem. Int. Ed.* 35 (1996) 2211.
- [5] W. Kahlen, H.H. Wagner, W.F. Hölderich, *Catal. Lett.* 54 (1998) 85.
- [6] S.B. Ogunwumi, T. Bein, *Chem. Commun.* (1997) 901.
- [7] M. Sabater, A. Corma, A. Domenech, V. Fornés, H. García, *Chem. Commun.* (1997) 1285.
- [8] G. Gbery, A. Zsigmond, K.J. Balkus Jr., *Catal. Lett.* 74 (2001) 77.
- [9] R.A. Sheldon, I.W.C.E. Arends, H.E.B. Lemmers, *Catal. Today* 41 (1998) 387.
- [10] C. Schuster, W.F. Hölderich, *Catal. Today* 60 (2000) 193.
- [11] R.F. Parton, I.F.J. Vankelecom, M.J.A. Casselman, *J. Am. Chem. Soc.* 116 (1994) 4746.
- [12] R.I. Kureshy, N.H. Khan, S.H.R. Abdi, I. Ahmad, S. Singh, R.V. Jasra, *J. Catal.* 221 (2004) 234.
- [13] K.J. Balkus Jr., M. Eissa, R. Levado, *J. Am. Chem. Soc.* 117 (1995) 10753.
- [14] K.J. Balkus Jr., A.K. Khanmamedova, K.M. Dixon, F. Bedioui, *Appl. Catal. A Gen.* 143 (1996) 159.
- [15] C. Baleizão, H. García, *Chem. Rev.* 106 (2006) 3987.
- [16] M. Alvaro, E. Carbonell, M. Esplá, H. García, *Appl. Catal. B Environ.* 57 (2005) 37.
- [17] K.O. Xavier, J. Chacko, K.K. Mohammed Yusuff, *Appl. Catal. B Gen.* 258 (2004) 251.
- [18] P. Gelin, Y.B. Taarit, C. Naccache, *J. Catal.* 59 (1979) 357.
- [19] S. Ernst, H. Disteldorf, X. Yang, *Microporous Mesoporous Mater.* 22 (1998) 457.
- [20] C. Heinrichs, W.F. Hölderich, *Catal. Lett.* 58 (1999) 75.
- [21] F. Algarra, M.A. Esteves, V. Fornés, H. García, J. Primo, *New J. Chem.* 22 (1998) 333.
- [22] Y. Tanamura, T. Uchida, N. Teramae, M. Kikuchi, K. Kusaba, Y. Onodera, *Nano Lett.* 1 (2001) 387.
- [23] Q. Huo, D.I. Margolese, U. Ciesla, P. Feng, T.E. Gier, P. Sieger, R. Leon, P.M. Petroff, F. Schüth, G.D. Stucky, *Nature* 368 (1994) 317.
- [24] M.J. Kim, R. Ryoo, *Chem. Mater.* 11 (1999) 487.
- [25] T.W. Kim, R. Ryoo, M. Kruk, K.P. Gierszal, M. Jaroniec, S. Kamiya, O. Terasaki, *J. Phys. Chem. B* 108 (2004) 11480.
- [26] J.M. Kim, Y. Sakamoto, Y.K. Hwang, Y.U. Kwon, O. Terasaki, S.E. Park, G.D. Stucky, *J. Phys. Chem. B* 106 (2002) 2552.
- [27] J. Fan, C.Z. Yu, J. Lei, Q. Zhang, T.C. Li, B. Tu, W.Z. Zhou, D.Y. Zhao, *J. Am. Chem. Soc.* 127 (2005) 10794.
- [28] C. Yu, Y. Yu, D.Y. Zhao, *Chem. Commun.* (2000) 575.
- [29] H.Q. Yang, J. Li, J. Yang, Z.M. Liu, Q.H. Yang, C. Li, *Chem. Commun.* (2007) 1086.
- [30] J.F. Larrow, E.N. Jacobsen, *J. Org. Chem.* 59 (1994) 2939.
- [31] M. Kruk, J.R. Matos, M. Jaroniec, *Colloids Surf. A Physicochem. Eng. Aspects* 241 (2004) 27.
- [32] Y. Sakamoto, M. Kaneda, O. Terasaki, D.Y. Zhao, J.M. Kim, G.D. Stucky, H.J. Shin, R. Ryoo, *Nature* 408 (2000) 449.
- [33] M. Kruk, V. Antochshuk, J.R. Matos, L.P. Mercuri, M. Jaroniec, *J. Am. Chem. Soc.* 124 (2002) 124.
- [34] G.J. Kim, D.W. Park, *Catal. Today* 63 (2000) 537.
- [35] L. Frunza, H. Kosslick, H. Landmesser, E. Höft, R. Fricke, *J. Mol. Catal. A Chem.* 123 (1997) 179.
- [36] D.A. Annis, E.N. Jacobsen, *J. Am. Chem. Soc.* 121 (1999) 4147.
- [37] S.E. Schaus, B.D. Brandes, J.F. Larrow, M. Tokunaga, K.B. Hansen, A.E. Gould, M.E. Furrow, E.N. Jacobsen, *J. Am. Chem. Soc.* 124 (2002) 1307.